ResearchGate

See discussions, stats, and author profiles for this publication at: https://www.researchgate.net/publication/223588984

Raman and DFT study of static, dynamic interactions and isotope effect in pyridazine+H2O/D2O systems

ARTICLE *in* VIBRATIONAL SPECTROSCOPY · MARCH 2009

Impact Factor: 2 · DOI: 10.1016/j.vibspec.2008.09.015

CITATIONS
5

READS
39

4 AUTHORS, INCLUDING:

Wolfgang Kiefer
University of Wuerzburg
878 PUBLICATIONS **9,837** CITATIONS
SEE PROFILE

Ranjan K Singh
Banaras Hindu University
71 PUBLICATIONS **506** CITATIONS
SEE PROFILE

Available from: Wolfgang Kiefer
Retrieved on: 23 January 2016

Vibrational Spectroscopy 49 (2009) 242–250

Contents lists available at ScienceDirect

Vibrational Spectroscopy

journal homepage: www.elsevier.com/locate/vibspec

Raman and DFT study of static, dynamic interactions and isotope effect in pyridazine + H_2O/D_2O systems

Deepa Singh [a], Animesh K. Ojha [b], W. Kiefer [c], Ranjan K. Singh [a,*]

[a] Department of Physics, Banaras Hindu University, Varanasi 221005, Uttar Pradesh, India
[b] Department of Physics and Meteorology, Indian Institute of Technology, Kharagpur 721302, India
[c] Institut für Physikalische Chemie, Universität Würzburg, Am Hubland D-97074, Germany

ARTICLE INFO

Article history:
Received 30 January 2008
Received in revised form 24 September 2008
Accepted 24 September 2008
Available online 9 October 2008

Keywords:
Blue shift
Isotope effect
Static and dynamic interaction
Hydrogen bond and vibrational dephasing

ABSTRACT

Polarized Raman and density functional theory (DFT) approach have been applied to study the static and dynamic properties of pyridazine (PRD) in H_2O(W) and D_2O(D) environment. The possible hydrogen bonded (HB) complexes of PRD with H_2O in gas phase and in the water solvation (using IEF-PCM and Onsager models) have been calculated using a B3LYP functional and 6-31+G(d,p)/6-311++G(d,p) basis sets. The static interaction in the PRD + H_2O complex leads to a blue shift in all the Raman modes of PRD and red shift in the O–H modes of water. The IEF-PCM solvation model gives the Raman wavenumbers closest to the experimental values. Raman spectra of ~962 and 1061 cm^{-1} mode of PRD in the mixture of PRD + H_2O and PRD + D_2O at different mole fractions of PRD (x) have been measured. A difference in the wavenumber shift of the two modes of PRD is observed experimentally when PRD is diluted with H_2O and D_2O. The wavenumber shift at maximum dilution ($x = 0.1$), however, takes the same value in both H_2O and D_2O. In view of the similar chemical properties of H_2O and D_2O, the difference in the trend of the wavenumber shift is not trivial. It has been explained on the basis of relative values of dipole moments of H_2O, D_2O, and conjugated molecules of PRD with H_2O/D_2O calculated theoretically and the role of larger diffusive property of H_2O compared to D_2O. The dynamical process in the mixture of PRD+ H_2O/D_2O is discussed by studying the variation of the linewidth with concentration. A theoretical model, which is based on the fact that the concentration in microscopic volume fluctuates, fits the experimental results nicely.

© 2008 Elsevier B.V. All rights reserved.

1. Introduction

The six-membered nitrogenated aromatic ring molecules such as diazines are the most studied [1–5] heterocyclic compounds. Diazines possess two different kinds of proton-accepter sites, one is the ring π cloud and another is the lone pairs on the nitrogen atoms. The lone pairs on nitrogen atoms of pyridazine are sp^2 hybridized and it is highly sensitive to protic solvents like water to form a hydrogen bond. The HB interaction plays an important role in determining the molecular conformation, crystal packing and the structure of biological systems. Many chemical and biochemical processes occur in solutions, which could be investigated by studying the solvated molecules [6–10]. A number of theoretical methods have been developed so far to study the solvation effect [9,10]. These can be classified in three categories; discrete model, in which both solvent and solute molecules are treated as separate units, which form small clusters of weakly bounded complexes of solvent and solute molecules. The second is continuum model, in which solvent is represented as a continuum dielectric medium that interacts with the solute molecule and the third one is the combination of discrete and continuum model.

Raman spectroscopy is also a very useful tool to study the intermolecular association in liquid mixtures [3,11–21]. A considerable amount of information about the vibrational relaxations and molecular association in molecular liquids can be obtained by analyzing the line shapes of the experimentally measured isotropic component of the Raman spectra [20,21]. The static and dynamic properties of the systems are determined by studying the variation of the peak position and the linewidth as a function of concentration in solution. Many semi-analytical theoretical models have also been proposed [22–26] to explain the variation of linewidth and peak position in solutions.

Several theoretical studies [27–31] of vibrational analysis of pyridazine using DFT methods have been reported. The rotational studies [32,33] of benzene + water complex reveal the water molecules situated above the benzene plane with both H atoms

* Corresponding author. Tel.: +91 542 6701569/9451272424 (Mobile).
E-mail address: ranjanksingh65@rediffmail.com (R.K. Singh).

0924-2031/$ – see front matter © 2008 Elsevier B.V. All rights reserved.
doi:10.1016/j.vibspec.2008.09.015

pointing towards the π cloud. π-complex benzene dimer structure through C–H···π bond is also proposed using ab initio methods [34]. The rotational spectra of 1:1 complexes of pyridazine + water [35], pyrazine + water [36] and pyrimidine + water [37] showed only a planer structure with a bent O–H···N hydrogen bond.

In view of the above discussions we have applied Raman + DFT approach to study the static and dynamic properties of PRD in H_2O and D_2O and to see how these properties differ in H_2O and D_2O. The three categories of solvation have been used to reach a more complete understanding of the nature of the interaction between the solute and the solvent. Different geometrical structures have been analyzed. Vibrational analysis of PRD and its complexes are also done to see the vibrational wavenumber shift. Two sharp, isolated and sufficiently intense Raman bands are selected for vibrational dephasing studies.

2. Experimental details

PRD, H_2O and D_2O obtained commercially from Aldrich with 99% purity were used without further purification. The parallel and perpendicular components of the Raman spectra in the region 950–1080 cm^{-1}, which contains two prominent bands of pyridazine, were recorded in the two solvents at different concentrations (Fig. 1a and b). The isotropic component of the Raman spectra was calculated by making a linear combination: $I_{iso} = I_{||} - (4/3)I_{\perp}$ at each concentration. A Spex 1404 double monochromator with grating constant 2100 grooves/mm and liquid N_2-cooled CCD detector were employed to record the spectra. The 514.5 nm line of an argon ion laser delivering ~50 MW power at the sample was used as excitation source. The depolarization ratios of the 459, 314 and 218 cm^{-1} bands were measured before the measurement of samples and they were found as < 0.01, 0.75 and 0.75, respectively. The entrance slit was kept at 50 μm in order to get sharp bands, which also adds to the accuracy in the measurement of the peak positions and linewidths. The Raman bands having linewidths of ~3 cm^{-1} and above have relatively small contribution from the instrumental slit function at this slit opening [21].

3. Computational details

All calculations were carried out using Gaussian03 [38] and the results were viewed by GaussView 4.1 [39] programme packages. We performed natural bond orbital (NBO) analysis with NBO 3.1 programme [40] for calculating the charges. Optimized gas phase PRD and PRD + nH_2O (n = 1, 2) complexes (Discrete model), PRD solvated in water (Continuum model) and PRD + nH_2O (n = 1, 2) complexes (combined model) solvated in water are shown in Fig. 2. Two solvation models, Onsager [41] and IEF-PCM [42,43], have been used. In the Onsager model the solute molecule occupies a fixed spherical cavity within the solvent field. The dipolar solute molecule induces a dipole moment in the medium and the electric field of the induced dipole in solvent will in turn interact with the dipolar solute molecule leading to the net stabilization. In the IEF-PCM solvation model, the solvent electrostatic reaction field is represented in terms of an apparent surface charge defined on the surface of the molecular cavity (i.e., the boundary between solute and solvent) surrounding a cavity with shape and dimension adjusted on the basis of the real geometric structure of the solute molecule. The latter polarizes the solvent, which, as a response, induces an electric field (the "reaction field") that interacts with the solute. The third is the combined discrete/continuum model [10]. Geometry optimization and frequency calculation for PRD and its complexes with one and two water molecules in gas phase and in water solvation were performed with density functional theory (DFT) using B3LYP functional with 6-31+G(d,p) and 6-311++G(d,p) basis sets [44,45]. The absence of negative wavenumber indicates that the optimized structures are at the minimum of the potential energy surface. The optimized structures with higher basis set are more energetically stable than those with the lower basis set.

3.1. Geometrical structures

Two water molecules are enough to saturate the two hydrogen bonding acceptor sites of PRD molecule [6]. Complexes of PRD

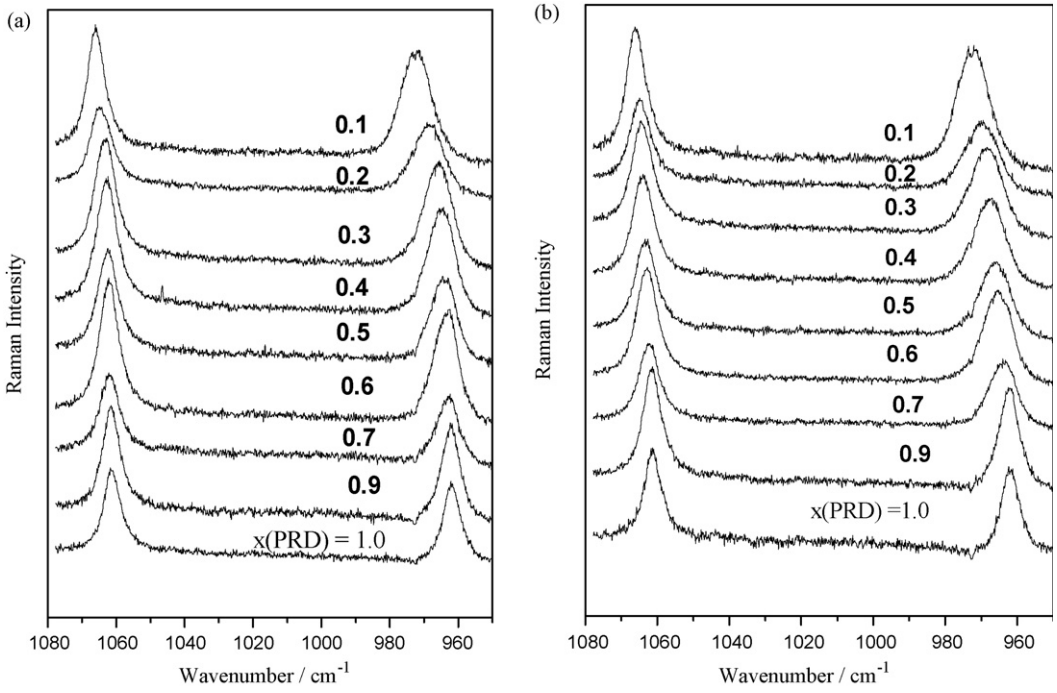

Fig. 1. Isotropic part of the Raman spectra of PRD in the region 950–1080 cm^{-1} at different mole fractions of PRD, x(PRD) in (a) PRD + H_2O and (b) PRD + D_2O mixtures.

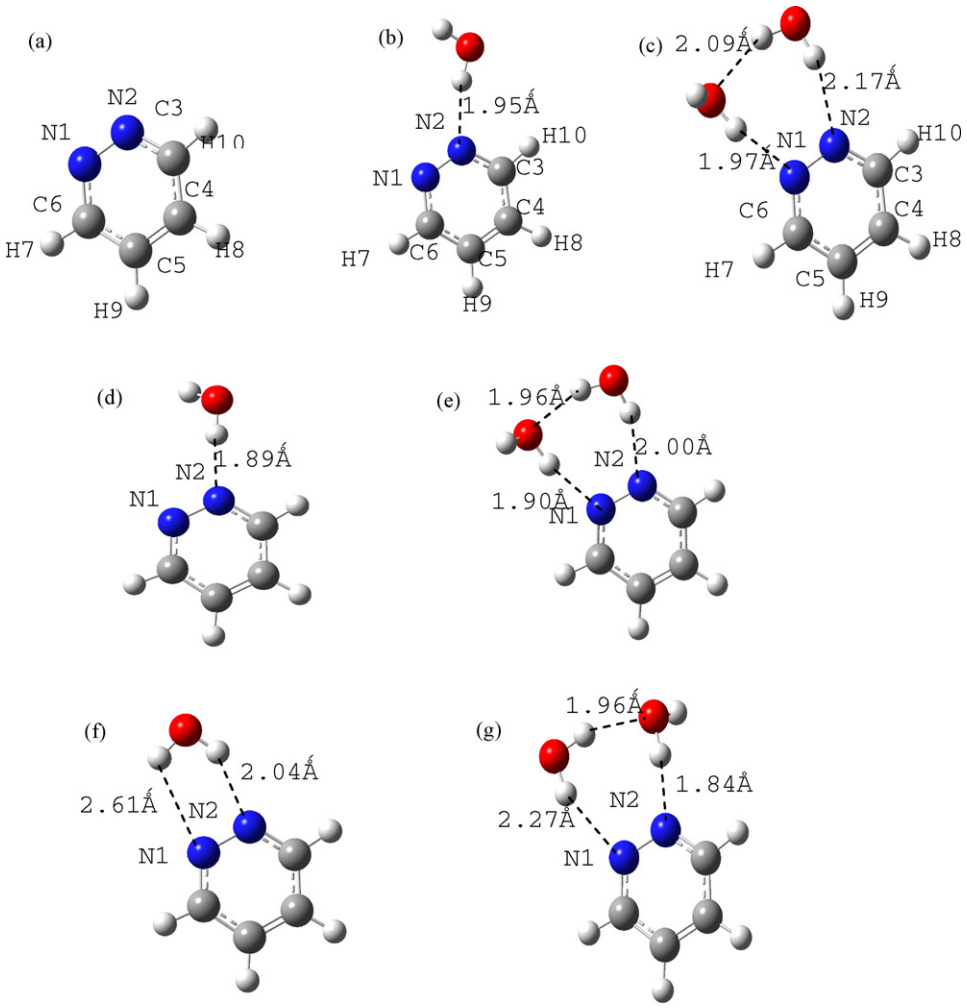

Fig. 2. Optimized structures of (a) gas phase PRD; (b) gas phase PRDW; (c) gas phase $PRDW_2$; (d) IEF-PCM solvated PRDW; (e) IEF-PCM solvated $PRDW_2$; (f) Onsager solvated PRDW; (g) Onsager solvated $PRDW_2$.

were therefore optimized with one/two water molecules only. We attached one water molecule with PRD in three configurations, first through N1 atom, second through N2 atom and finally in the π-shaped form but the optimization resulted into the same structure, where water molecule is attached to the N2 atom in a planer structure with a bent N···H–O H-bond (Fig. 2b) is formed. In contrast to the benzene + water complex [32,33], where water molecule lies above the ring plane through O–H···π hydrogen bond, all three diazines form planer complexes with water molecule through N···H–O hydrogen bond [35]. The gas phase complexes (Fig. 2b and c) are reoptimized in the water solvation (Fig. 2d–g). Two N···H–O and one O···H–O type H-bonds form a closed cyclic structure of seven atoms in $PRDW_2$ (Fig. 2c). The H-bond lengths of PRDW and $PRDW_2$ in gas phase and in solvation for both basis sets are given in Table 1. The geometrical parameters of PRD in HB complexes are almost same to that of the free PRD. H-bond length is smaller in the continuum model than the gas phase (Table 1). The NBO charges on each atom of PRD in pure and in HB complexes are given in the Tables 2–4 for gas phase, Onsager and IEF-PCM solvation, respectively. The effect of basis set superposition error (BSSE) was analyzed in the optimized complexes using the standard counterpoise (CP) method [46]. The effects of CP corrections are negligible on both geometrical parameters and the binding energy of the PRD. On CP correction, however, the H-bond length slightly increases.

The structure of PRD, PRDW and $PRDW_2$ are similar in the gas phase and the IEF-PCM solvation model, whereas the structure of the complexes is different in the Onsager solvation model as

Table 1
H-bond lengths (Å) of PRDW and $PRDW_2$ in gas phase, and in IEF-PCM and Onsager solvation models calculated at B3LYP/6-31+G(d,p) and 6-311++G(d,p) levels of theory.

Bonds	Gas		IEF-PCM		Onsager	
	PRDW	$PRDW_2$	PRDW	$PRDW_2$	PRDW	$PRDW_2$
	6-31+G(d,p) (6-311++G(d,p))	6-31+G(d,p) (6-311++G(d,p))	6-31+G(d,p) (6-311++G(d,p))	6-31+G(d,p) (6-311++G(d,p))	6-31+G(d,p) (6-311++G(d,p))	6-31+G(d,p) (6-311++G(d,p))
N1···H	–	1.96 (1.97)	–	1.88 (1.90)	– (2.61)	2.29 (2.27)
N2···H	1.94 (1.95)	2.18 (2.17)	1.88 (1.89)	2.00 (2.00)	1.99 (2.04)	1.85 (1.84)
O···H	–	2.08 (2.09)	–	1.95 (1.96)	–	1.96 (1.96)

The values given in the parenthesis ( ) are with 6-311++G(d,p).

Table 2
NBO charges (the atomic charge unit) on atoms of PRD in pure PRD, PRDW and $PRDW_2$ in the gaseous phase at the B3LYP/6-31+G(d,p) and B3LYP/6-311++G(d,p) theory level.

Atoms	PRD		PRDW		$PRDW_2$	
	6-31+G(d,p)	6-311++G(d,p)	6-31+G(d,p)	6-311++G(d,p)	6-31+G(d,p)	6-311++G(d,p)
N1	−0.233	(0.230	(0.223	(0.219	(0.275	(0.278
N2	(0.233	(0.230	(0.269	(0.276	(0.248	(0.248
C3	(0.024	0.019	(0.006	0.037	(0.004	0.038
C4	(0.246	(0.205	(0.241	(0.200	(0.232	(0.191
C5	(0.246	(0.205	(0.239	(0.198	(0.236	(0.195
C6	(0.024	0.019	(0.019	0.024	0.000	0.042
H7	0.245	0.199	0.249	0.202	0.254	0.208
H8	0.257	0.217	0.262	0.221	0.265	0.224
H9	0.257	0.217	0.260	0.220	0.265	0.224
H10	0.245	0.199	0.258	0.213	0.256	0.210
Net charge	**0.000**	**0.000**	**0.032**	**0.026**	**0.044**	**0.033**

Table 3
NBO charges (the atomic charge unit) on atoms of PRD in pure PRD, PRDW and $PRDW_2$ in the Onsager solvation calculated at the B3LYP/6-31+G(d,p) and B3LYP/6-311++G(d,p) levels.

Atoms	PRD		PRDW		$PRDW_2$	
	6-31+G(d,p)	6-311++G(d,p)	6-31+G(d,p)	6-311++G(d,p)	6-31+G(d,p)	6-311++G(d,p)
N1	(0.256	(0.253	(0.259	(0.256	(0.275	(0.274
N2	(0.256	(0.253	(0.297	(0.303	(0.306	(0.312
C3	0.024	0.020	(0.006	0.039	0.006	0.049
C4	(0.235	(0.193	(0.230	(0.188	(0.217	(0.175
C5	(0.235	(0.193	(0.222	(0.180	(0.217	(0.175
C6	(0.024	0.020	(0.012	0.031	(0.005	0.036
H7	0.244	0.197	0.253	0.206	0.250	0.204
H8	0.271	0.230	0.277	0.236	0.289	0.247
H9	0.271	0.230	0.280	0.239	0.284	0.242
H10	0.244	0.197	0.247	0.202	0.257	0.211
Net charge	**0.000**	**0.000**	**0.032**	**0.023**	**0.066**	**0.054**

shown in the Fig. 2. In the gas phase PRDW structure, one O–H bond of H_2O is free and the other forms N···H–O, H-bond. The free O–H bond is shortened whereas the other involved in H-bond is elongated. In the PRDW complex (Onsager solvation model Fig. 2f) the water molecule is attached in such a way that two N···H–O H-bonds are formed. Both O–H bonds are elongated since they are involved in the H-bond. The $PRDW_2$ structure (Fig. 2g) obtained by Onsager model results in the water molecules rotated by 90° compared to IEF-PCM/gas phase structures. Due to this rotation O–H bond of one water molecule is free while in the gas phase and the IEF-PCM solvated structure the O–H bond of the other water molecule is free. The free O–H bond is shortened and the O–H bond participating in the H-bond is elongated in the complexes in gas phase and in solvation both.

3.2. Vibrational analysis

Some prominent Raman active modes in gas phase and in water solvation along with the dipole moments are reported in the Tables 5–7. Due to the negligence of anharmonicity effects and the approximate treatment of the electron correlation in DFT calculations, vibrational wavenumbers are typically larger than those observed experimentally [6]. We have reported the unscaled wavenumbers in view of the fact that the scaling factors [47] have been obtained through fitting procedures on gas phase data, which

Table 4
NBO charges (the atomic charge unit) on atoms of PRD in pure PRD, PRDW and $PRDW_2$ in the IEF-PCM solvation calculated at the B3LYP/6-31+G(d,p) and B3LYP/6-311++G(d,p) levels.

Atoms	PRD		PRDW		$PRDW_2$	
	6-31+G(d,p)	6-311++G(d,p)	6-31+G(d,p)	6-311++G(d,p)	6-31+G(d,p)	6-311++G(d,p)
N1	(0.294	(0.292	(0.278	(0.275	(0.302	(0.307
N2	(0.294	(0.292	(0.308	(0.314	(0.294	(0.297
C3	(0.021	0.022	(0.004	0.039	(0.001	0.041
C4	(0.236	(0.196	(0.234	(0.193	(0.228	(0.187
C5	(0.236	(0.196	(0.231	(0.190	(0.229	(0.188
C6	(0.021	0.022	(0.016	0.026	0.002	0.044
H7	0.267	0.221	0.269	0.224	0.274	0.229
H8	0.285	0.244	0.287	0.247	0.289	0.249
H9	0.285	0.244	0.287	0.247	0.289	0.249
H10	0.267	0.221	0.271	0.226	0.273	0.228
Net charge	**0.000**	**0.000**	**0.044**	**0.036**	**0.074**	**0.060**

Table 5
Wavenumbers of some prominent Raman bands (cm^{-1}) and dipole moment (in Debye) of PRD, PRDW, $PRDW_2$ and H_2O in gas phase with B3LYP/6-31+G(d,p) and 6-311++G(d,p).

PRD		Expt [29]; IR/Raman	Discrete model				Assignments [49]
6-31+G(d,p)	6-311++G(d,p)		PRDW		$PRDW_2$		
			6-31+G(d,p)	6-311++G(d,p)	6-31+G(d,p)	6-311++G(d,p)	
631.2	634.3	629/630	638.9	642.5	641.3	644.5	δ ring 3 (92.7)
680.3	681.3	664/667	682.6	683.1	681.7	682.3	δ ring 2 (90.0)
1013.3	1008.6	963/964	1017.8	1014.6	1019.7	1015.3	$\gamma(CH)'_{as}(105.5) + \gamma(CH)_{as}(13.5)$
1095.2	1090.1	1061/1063	1096.6	1093.9	1097.9	1093.5	ν(C4C5)(41.0) + $\delta(CH)_s(22.6) + \nu(NN)(22.1) + \nu(CC)_s(12.2)$
1174.3	1171.3	1131/1129	1177.7	1176.5	1179.5	1178.4	$\delta(CH)'_s(59.2) + \delta(CH)_s(16.4) + \nu(NN)(13.6) + \nu(NC)_s(10.5)$
1199.2	1180.8	1159/1160	1213.9	1192.2	1222.7	1202.6	$\nu(NC)_s(62.1) + \nu(CC)_s(21.0) + \delta(CH)'_s(10.4)$
1610.4	1602.2	1563/1566	1615.9	1606.1	1617.9	1609.1	$\nu(CC)_{as}(44.3) + \delta(CH)'_{as}(24.4) + \nu(NC)_{as}(22.7)$
1615.6	1606.9	1570/1572	1617.8	1609.0	1619.8	1610.7	ν(C4C5)(46.8) + $\delta(CH)_s(18.9)$
3187.8	3167.9	3056/3052	3194.5	3173.1	3198.6	3177.6	$\nu(CH)'_{as}(97.3)$
3193.7	3173.1	3056/3050	3201.6	3179.8	3204.2	3182.5	$\nu(CH)'_s(80.0) + \nu(CH)_s(19.7)$
3203.6	3184.5	3068/3064	3210.1	3189.4	3213.2	3192.7	$\nu(CH)_{as}(97.0)$
3214.9	3196.9	3085/3083	3220.3	3201.2	3223.0	3204.0	$\nu(CH)_s(79.5) + \nu(CH)'_s(19.6)$
–	–		3576.7	3818.7	3716.7	3725.1	$\nu(O–H)_s$
–	–		3888.6	3923.8	3795.3	3786.4	$\nu(O–H)_{as}$
–	–		–	–	3567.6	3574.1	$\nu(O–H)_s$
–	–		–	–	3885.1	3882.4	$\nu(O–H)_{as}$
4.42	4.42		6.07	5.53	9.02	8.96	Dipole moment

Table 6
B3LYP/6-31+G(d,p) and 6-311++G(d,p) wavenumbers (cm^{-1}) of some prominent Raman bands of PRD in IEF-PCM and Onsager solvation (Continuum model) and dipole moment (in Debye) of PRD.

IEF-PCM		Onsager		Assignments [49]
6-31+G(d,p)	6-311++G(d,p)	6-31+G(d,p)	6-311++G(d,p)	
631.5	634.8	631.2	634.4	δ ring 3 (92.7)
674.9	677.3	681.3	682.3	δ ring 2 (90.0)
1004.8	998.3	1009.6	1005.0	$\gamma(CH)'_{as}(105.5) + \gamma(CH)_{as}(13.5)$
1087.6	1082.9	1094.7	1089.9	ν(C4C5)(41.0) + $\delta(CH)_s(22.6) + \nu(NN)(22.1) + \nu(CC)_s(12.2)$
1162.1	1159.4	1179.0	1177.1	$\delta(CH)'_s(59.2) + \delta(CH)_s(16.4) + \nu(NN)(13.6) + \nu(NC)_s(10.5)$
1220.3	1202.6	1206.7	1188.1	$\nu(NC)_s(62.1) + \nu(CC)_s(21.0) + \delta(CH)'_s(10.4)$
1608.5	1599.0	1611.0	1602.0	$\nu(CC)_{as}(44.3) + \delta(CH)'_{as}(24.4) + \nu(NC)_{as}(22.7)$
1611.7	1604.0	1616.0	1606.9	ν(C4C5)(46.8) + $\delta(CH)_s(18.9)$
3130.0	3109.5	3191.0	3169.2	$\nu(CH)'_{as}(97.3)$
3134.6	3113.5	3194.6	3172.6	$\nu(CH)'_s(80.0) + \nu(CH)_s(19.7)$
3143.0	3123.2	3210.2	3190.1	$\nu(CH)_{as}(97.0)$
3151.5	3132.8	3222.0	3202.5	$\nu(CH)_s(79.5) + \nu(CH)'_s(19.6)$
6.31	6.31	5.38	5.37	Dipole moment

Table 7
B3LYP/6-31+G(d,p) and 6-311++G(d,p) calculated frequencies (cm^{-1}) of some prominent Raman bands of PRDW and $PRDW_2$ and dipole moment (in Debye) in combined solvation model.

IEF-PCM				Onsager			
PRDW		$PRDW_2$		PRDW		$PRDW_2$	
6-31+G(d,p)	6-311++G(d,p)	6-31+G(d,p)	6-311++G(d,p)	6-31+G(d,p)	6-311++G(d,p)	6-31+G(d,p)	6-311++G(d,p)
639.6	644.8	644.8	647.7	636.0	638.7	641.4	644.9
680.1	682.3	682.2	683.1	683.5	685.3	684.5	685.9
1009.4	1004.2	1009.4	1004.9	1011.1	1001.0	1013.0	1006.7
1090.4	1086.2	1089.4	1085.0	1094.9	1089.5	1098.6	1095.8
1163.3	1161.8	1163.9	1162.6	1183.0	1185.3	1186.4	1187.4
1232.1	1212.6	1241.7	1221.9	1224.7	1212.4	1235.9	1220.1
1613.8	1602.6	1614.2	1602.0	1615.0	1604.2	1616.2	1606.4
1618.3	1605.3	1616.1	1606.0	1618.2	1609.6	1620.1	1611.2
3134.1	3109.5	3133.5	3110.9	3197.8	3177.0	3201.9	3179.8
3138.5	3113.5	3137.5	3114.5	3203.0	3181.5	3205.9	3184.2
3146.6	3123.2	3146.0	3124.3	3216.4	3197.4	3219.2	3198.7
3155.1	3132.8	3154.5	3133.8	3227.0	3207.8	3229.0	3208.6
3424.5	3431.2	3572.0	3576.2	3564.9	3579.2	3658.1	3661.2 ($\nu(O–H)_s$)
3670.5	3672.4	3657.8	3661.0	3865.6	3832.1	3741.8	3710.2 ($\nu(O–H)_{as}$)
–	–	3399.8	3420.3	–	–	3658.1	3661.2 ($\nu(O–H)_s$)
–	–	3641.1	3643.6	–	–	3741.8	3710.2 ($\nu(O–H)_{as}$)
8.21	8.14	11.54	11.45	8.85	9.86	11.89	12.38 (dipole moment)

may not be valid for solvated systems [6,48]. The experimental values of IR and Raman wavenumbers from an earlier study [29] are also given in the Table 5 for the sake of comparison. Assignments of vibrational bands are reported from the work of Brede et al. [49]. The IEF-PCM continuum model with 6-311++G(d,p) basis set gives the computed wavenumbers closest to the experimental values. This is also true for the two bands at 962.2 and 1061.8 cm^{-1} for which concentration dependent Raman study have been done. These two bands are assigned as $\gamma(CH)'_{as}(85.5) + \gamma(CH)_{as}(13.5)$ and $\nu(C4C5)(41.0) + \delta(CH)_s(22.6) + \nu(NN)(22.1) + \nu(CC)_s(12.2)$, respectively [29]. No new band is observed experimentally corresponding to these two bands when diluted with water. It suggests that the interaction of PRD molecule with the bulk of the solvent is more effective than the interaction between individual PRD and solvent molecules. All the reported modes are blue shifted on complex formation in both gas phase and in solvation except the two modes at 1005.0 and 1089.5 cm^{-1} of PRDW (6-311++G(d,p)) by Onsager model as shown in Table 6.

The two experimentally reported bands at 962.2 and 1061.8 cm^{-1} in pure PRD shift by 10 and 4 cm^{-1}, respectively, on highest dilution. The peak position at highest dilution (972.5 cm^{-1}) can be compared with that in solvation. It appears theoretically at 1009.7 and 1004.9 cm^{-1} with Onsager and IEF-PCM models, respectively, using the B3LYP/6-31+G(d,p) basis set. On applying B3LYP/6-311++G(d,p) basis set the same mode appears at 1005.0 and 998.4 cm^{-1} with the Onsager and IEF-PCM models, respectively.

3.3. C–H stretching

The C–H bond lengths of PRD are reduced on average by 0.4% on complex formation with water molecules. The C–H bonds are not involved in H-bond; nevertheless the C–H stretching modes are blue shifted and force constant increases on complex formation in both gas phase and in solvation. Many cases of blue shift (improper hydrogen bond) of the C–H stretching mode (involved in hydrogen bond) have been reported [50,51] in last 10 years. The possible cause of blue shifting of C–H modes involved in hydrogen bonding is electrostatic interaction. The blue shift of the C–H stretching modes in present case is, however, different from the improper hydrogen bonding where the blue shifted C–H modes are directly involved in the hydrogen bond. When complexes of PRD are formed, redistribution of charge takes place and causes some charge transfer from water to PRD molecule. The charge transfer is more when the number of water molecules in the complex is more (see Tables 2–4). The pure PRD is neutral molecule. In PRDW and $PRDW_2$ the net absolute charge on PRD is 0.032e and 0.042e respectively. This additional charge on PRD in PRDW and $PRDW_2$ is due to the charge transferred from water molecule to PRD. The transfer of charge from water molecules to the PRD atom might be a possible cause of the blue shift in modes of PRD on complex formation.

3.4. O–H stretching

In N···H–O hydrogen bond, the O–H stretching frequency is red shifted on complex formation. The calculated frequency shift of the symmetric and antisymmetric O–H stretching mode for PRDW and $PRDW_2$ are reported in Tables 5 and 7. The frequency shift of the symmetric/antisymmetric O–H stretching mode is large. The charge transfer from water to PRD might be responsible for this large shift. There are only two bonds in water molecule. The charge transferred from two bonds is distributed on many bonds of PRD. Simultaneous red shift in modes of water and blue shift in modes of PRD are therefore observed.

4. Difference in wavenumber shift of the 962 and 1061 cm^{-1} bands in the mixture of pyridazine + H_2O/D_2O: effect of dipole moment and diffusion

The maximum shift of the wavenumber of the 962 cm^{-1} ($\Delta\omega \cong 10$ cm^{-1}) and 1061 cm^{-1} ($\Delta\omega \cong 4$ cm^{-1}) (Table 8) is the same in case of both H_2O and D_2O. The concentration dependence of the wavenumber shift of both the modes, however, follows different trends as shown in Fig. 3a and b. In order to present this aspect more clearly the difference in peak positions of the two modes in H_2O and D_2O has been plotted with concentration in Fig. 3c. The difference is maximum at $x = 0.35$.

Although the chemical properties of heavy water (D_2O) do not differ from those of water (H_2O), there are many other properties, which are affected due to the substitution of hydrogen by deuterium [52]. From the structural point of view, it is known that D_2O is slightly more ordered than H_2O [53]. A qualitative explanation of the difference in wavenumber shift at intermediate concentrations can be given in terms of the dipole moments of PRD, H_2O, D_2O, $PRDW_2$ and $PRDD_2$ and the difference in the diffusion coefficient of H_2O and D_2O. The dipole moments of H_2O and D_2O turn out to be 2.2 and 2.4 Debye, respectively, in our calculation. In another study [52] the same value of dipole moment of D_2O is reported, i.e. 2.4 Debye. The experimentally observed value of the dipole moment of D_2O is 2.3 Debye [52]. The complexes $PRDW_2$ and $PRDD_2$ are more polar having dipole moments 9.01 and 9.04 Debye, respectively. When H_2O or D_2O is mixed with PRD, at higher mole fractions, few of the PRD molecules are hydrogen bonded with H_2O/D_2O molecules. Since

Table 8
Observed vibrational wavenumbers (ν) and linewidths (FWHM($\Delta\nu_{1/2}$)$_R$) in cm^{-1} of two bands of PRD at ~962 and 1061 cm^{-1} in H_2O and D_2O at different mole fractions of PRD in PRD + H_2O/D_2O.

Concentration (mole fraction)	PRD + H_2O				PRD + D_2O			
	962 cm^{-1} band		1061 cm^{-1} band		962 cm^{-1} band		1061 cm^{-1} band	
	ν	$(\Delta\nu_{1/2})_R$	ν	$(\Delta\nu_{1/2})_R$	ν	$(\Delta\nu_{1/2})_R$	ν	$(\Delta\nu_{1/2})_R$
1.0	962.22	6.04	1061.75	5.50	962.22	6.04	1061.75	5.50
0.9	962.51	6.52	1062.04	5.55	962.28	7.02	1062.02	6.16
0.7	963.39	7.51	1062.46	6.50	964.07	9.28	1062.28	6.81
0.6	963.54	8.68	1062.46	6.37	965.46	10.05	1062.87	7.14
0.5	964.44	9.02	1062.65	6.61	966.23	10.31	1063.22	7.24
0.4	965.30	9.70	1062.94	6.84	967.78	10.85	1063.90	7.15
0.3	965.88	9.65	1063.22	7.05	968.59	11.16	1064.19	7.08
0.2	968.32	10.95	1064.95	7.63	969.94	11.38	1064.75	6.88
0.1	972.50	11.32	1065.80	5.80	972.32	10.75	1065.90	6.48

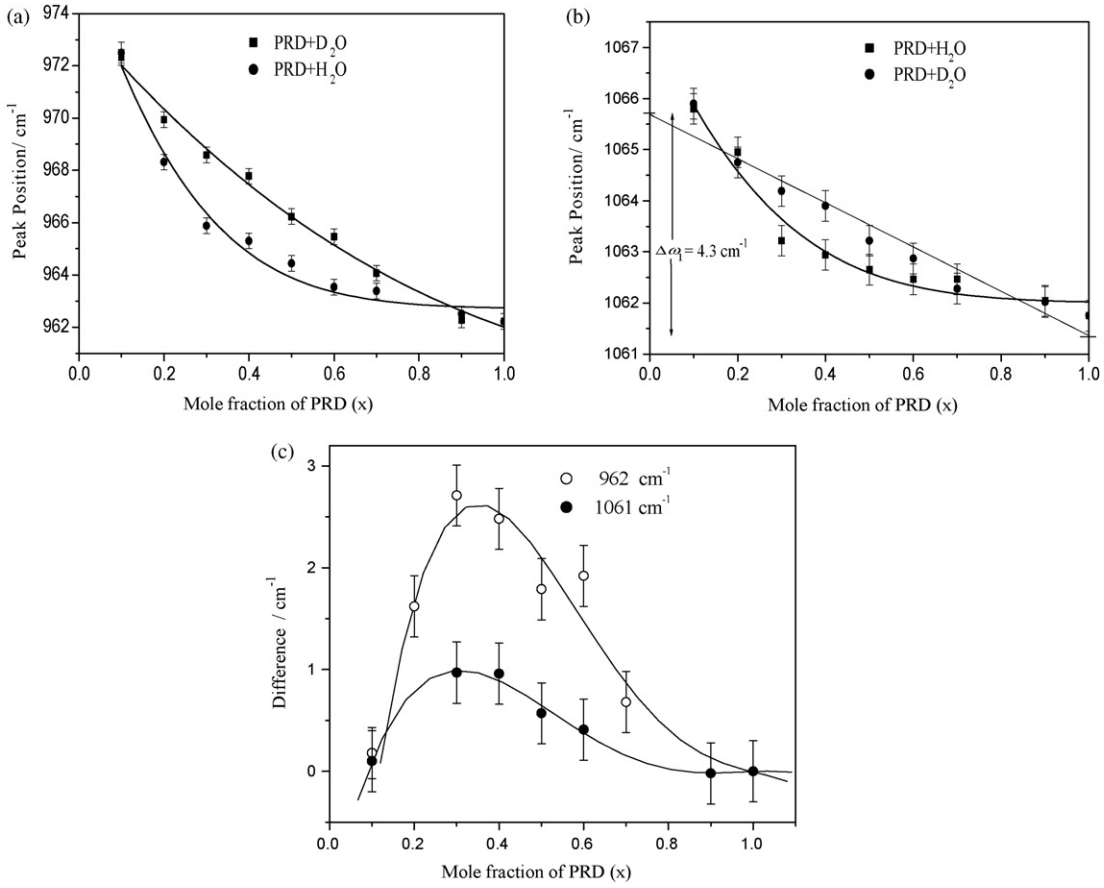

Fig. 3. Variation of the peak position of (a) the 962 cm^{-1} band in PRD + H_2O and PRD + D_2O and (b) the 1061 cm^{-1} band in PRD + H_2O and PRD + D_2O with concentration of PRD in mole fraction (c) plot of difference in the wavenumbers of the 962 and 1061 cm^{-1} bands in PRD + H_2O and PRD + D_2O with concentration of PRD in mole fraction.

the HB species have higher dipole moments, there are centers of higher dipole moment molecules in the solution. D_2O being heavier requires more energetic hydrogen bonds for the complex to be stable. In the mixtures of higher mole fractions of PRD, it is therefore expected that the number of conjugated molecules are more in H_2O than that in D_2O. On increasing the amount of H_2O/D_2O in the mixture (i.e. increasing the mole fraction of PRD in the mixture) the difference in the number of HB PRD molecules increases. More difference in the number of polar complex molecules at higher and intermediate concentrations of PRD ($x > 0.35$) causes more difference in the peak position. On increasing the amount of H_2O/D_2O in the solution (i.e. going to lower mole fraction of PRD), diffusion becomes more and more effective. The diffusion coefficient of D_2O is about 20% lower than that of H_2O [52]. Larger diffusion of H_2O reduces the number of conjugated molecules of PRD. At concentrations less than 0.35 more diffusion of water molecules in the solution causes the hydrogen bonds to rupture leading to almost equal number of conjugated molecules in H_2O and D_2O. The resultant effect of heavier D_2O and more diffusion of H_2O lead to same number of complexes with H_2O and D_2O at highest dilution. The difference does not increase further but approaches to zero at $x = 0.1$. The relative effect of heavy water in comparison with ordinary water on spectral parameters is larger than that expected by mere difference in masses [54]. In conclusion we believe that the difference in wavenumber shift with H_2O and D_2O at a particular concentration is a function of the difference of conjugated molecules in H_2O and D_2O.

5. Dynamic processes in the mixture of pyridazine + H_2O/D_2O: effect concentration inhomogeneities

The linewidths of the 962 and 1061 cm^{-1} bands of PRD are plotted with concentration in mole fractions of PRD in the mixture of PRD + H_2O/D_2O in Fig. 4a and b, respectively. The linewidth of the 962 cm^{-1} band in water increases linearly whereas in D_2O it increases from 6 to 11 cm^{-1} becoming maximum at $x = 0.3$ (Fig. 4a) and decreasing on further dilution. The linewidth of the 1061 cm^{-1} band also increases linearly in water solvent (Fig. 4b). In D_2O the 1061 cm^{-1} band on the other hand shows a curve like variation in linewidth peaking at $x = 0.5$ and decreasing on further dilution. A similar type of variation in linewidth has been proposed due to concentration fluctuation [22]. This type of variation of linewidth is based on the proposition that the low lying hydrogen bridging mode is anharmonically coupled with a higher wavenumber mode and causes the wavenumber and linewidth to change. The concentration in a microscopic volume of the mixture fluctuates leading to the maximum linewidth when the number of molecules of reference and solvent system are equal in the mixture [21]. In solution the other important cause of line broadening is diffusion. In the present systems PRD + H_2O/D_2O the low lying hydrogen bridging mode (N···H stretching mode) is anharmonically coupled with a higher wavenumber mode and causes the wavenumber and linewidth to change. Due to larger diffusion of water the effect of concentration fluctuation is smeared out in H_2O solvent and the increase in linewidth is

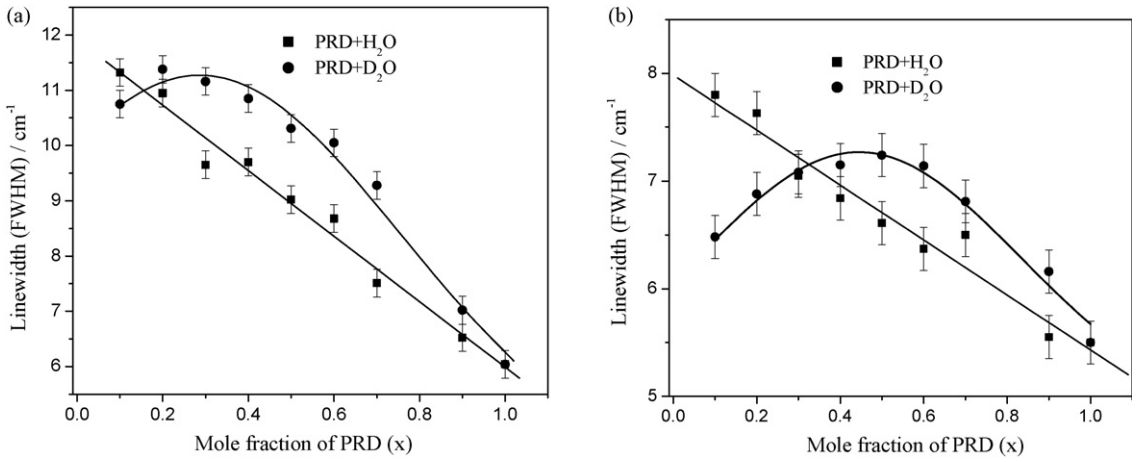

Fig. 4. Variation of the linewidth of (a) the 962 cm^{-1} band in PRD + H_2O and PRD + D_2O and (b) the 1061 cm^{-1} band in PRD + H_2O and PRD + D_2O with concentration of PRD in mole fraction.

linear. The linewidth vs. concentration curve of the 962 cm^{-1} of D_2O peaks at $x = 0.3$ (not at $x = 0.5$) and it indicates the influence of concentration fluctuation but due to the shift of its position from $x = 0.5$–0.3, the effect of diffusion seems to be present effectively in this mode.

The linewidth of 1061 cm^{-1} band in D_2O shown in Fig. 4b peaks at $x = 0.5$. The same trend in the variation of linewidth has been reported experimentally in the pyridine + methanol system [11,21], acrylonitrile + methanol system [55] and chlorobenzene + methanol system [16]. Very recently an empirical model based on the relative viscosity which is in fact an extension of concentration fluctuation model has been proposed [56]. This model can also reproduce the concentration dependence of linewidth. We, however, have applied the concentration fluctuation model [21,22] which proposes a linear variation of peak wavenumber with concentration in binary mixture as

$$\nu(x) = \nu_0 + X\,\Delta\omega_1, \tag{1}$$

where x is the concentration of the reference system expressed in mole fraction and $\Delta\omega_1$ is the amplitude of the wavenumber shift between the neat liquid and infinite dilution as shown in Fig. 3b. The wavenumber of 1061 cm^{-1} band of PRD in D_2O increases linearly with concentration (Fig. 3b). The random motion of PRD and D_2O molecules in the mixture causes the concentration in the microvolume to fluctuate around a mean value and leads to a linewidth variation peaking at x (PRD) = 0.5 (Fig. 4b) given by the relationship:

$$\Gamma_x = 2(2\ln 2)^{1/2}\,\Delta\omega_1\left[\frac{x(1-x)}{n}\right]^{1/2}, \tag{2}$$

where n is the number of the neighboring molecules influencing the reference mode. In the present system a weak hydrogen bond influences the 1061 cm^{-1} mode. One molecule of PRD is attached to 3.5 water molecules on an average [57]. By substituting the value of $\Delta\omega_1 = 4.3$ cm^{-1} (Fig. 3b) and $n = 4$ in Eq. (2), Γ_x is calculated to be 2.54 cm^{-1}. Considering the contributions to the linewidth from concentration fluctuation, Γ_x and intrinsic linewidth, Γ_i to be additive, the total linewidth at concentration x, $\Gamma(x)$ can be expressed as

$$\Gamma(x) = \Gamma_x + \Gamma_i \tag{3}$$

$\Gamma(x)$ is found to be 7.24 cm^{-1} for the 1061 cm^{-1} band at $x = 0.5$. The intrinsic linewidth, Γ_i at $x = 0.5$ is estimated to be 4.7 cm^{-1} using Eq. (3). Following the concepts of the indirect dephasing model, Fischer and Laubereau [23] proposed that the intrinsic linewidth Γ_i can be given as

$$\Gamma_i = 2\pi c(\Delta\omega_1)^2 T_1 \exp(\beta\omega_2) \tag{4}$$

ω_2 is the wavenumber of the hydrogen bridging N···H stretching mode (145 cm^{-1} calculated theoretically) and $\beta = 1/kT$, where C is the speed of light, k is the Boltzmann constant and $T = 300$ K (room temperature). T_1 is the dephasing time. The wavenumber shift $\Delta\omega_1$, Γ_i and ω_2 when substituted in Eq. (4) gives the vibrational dephasing time 0.013 ps.

6. Conclusions

A Raman study of vibrational dephasing of the 962 and the 1061 cm^{-1} bands in H_2O and D_2O environment has been performed. In order to explain the experimental results, quantum chemical calculation to obtain the optimized geometry and vibrational wavenumbers of PRD and its complexes with H_2O molecules has been done in gas phase and in the water environment. The two possible complexes of PRD with one/two H_2O or D_2O are possible. Experimental results match more closely with the theoretically calculated wavenumbers obtained from the continuum model. All the Raman modes of PRD are blue shifted and the O–H modes of water are red shifted on conjugation. The electronic charge shift from water molecule to PRD molecule is expected to be one of the possible causes for the blue/red shift. The experimentally observed blue shifts in the 962 and the 1061 cm^{-1} bands are 10 and 4 cm^{-1}, respectively. The shift in wavenumber and line width of PRD is found to be different in H_2O and D_2O solvent. The wavenumber shifts and linewidth changes are observed to be the same at high dilution with H_2O and D_2O. This difference is explained on the basis of larger dipole moment of $PRDW_2$ and the larger diffusion coefficient of H_2O than D_2O. The variation of linewidth and peak position of the 1061 cm^{-1} band in D_2O can be explained very nicely by concentration fluctuation model. The vibrational dephasing time for 1061 cm^{-1} band following this model using linear Raman data turns out to be 0.25 ps.

Acknowledgements

RKS is grateful to DST, India, for financial support. DS and RKS are grateful to UGC India for financial support. AKO and RKS are grateful to AvH foundation, Germany.

Appendix A. Supplementary data

Supplementary data associated with this article can be found, in the online version, at doi:10.1016/j.vibspec.2008.09.015.

References

[1] P.R. Rablen, J.W. Lockman, W.L. Jorgensen, J. Phys. Chem. A 102 (1998) 8097.
[2] A. Dkhissi, L. Adamowicz, G. Maes, J. Phys. Chem. A 104 (2000) 2112.
[3] S. Schlücker, R.K. Singh, B.P. Asthana, J. Popp, W. Kiefer, J. Phys. Chem. A 105 (2001) 9983.
[4] B. Zhang, Y. Cai, X.L. Mu, N.Q. Lou, X.Y. Wang, J. Chem. Phys. 117 (2002) 3701.
[5] D.Q. Xie, J. Zeng, J. Comput. Chem. 25 (2004) 1487.
[6] B. Mennucci, J.M. Martinez, J. Phys. Chem. B 109 (2005) 9818.
[7] G.P. Vitorino, G.D. Barrera, M.R. Mazzieri, R.C. Binning Jr., D.E. Bacelo, Chem. Phys. Lett. 432 (2006) 538–544.
[8] J. Tomasi, B. Mennucci, R. Cammi, Chem. Rev. 105 (2005) 2999–3094.
[9] B. Mennucci, J. Am. Chem. Soc. 124 (2002) 1506.
[10] F. Rodriguez-Ropero, J. Casanovas, C. Aleman, Chem. Phys. Lett. 416 (2005) 331–335.
[11] B.P. Asthana, H. Takahashi, W. Kiefer, Chem. Phys. Lett. 94 (1983) 41.
[12] V. Deckert, B.P. Asthana, P.C. Mishra, W. Kiefer, J. Raman Spectrosc. 27 (1996) 907.
[13] M.I. Cabaco, M. Besnard, Yarwood, J. Mol. Phys. 75 (1992) 139.
[14] M.I. Cabaco, M. Besnard, Yarwood, J. Mol. Phys. 75 (1992) 157.
[15] R.K. Singh, B.P. Asthana, A.L. Verma, C.M. Pathak, Chem. Phys. Lett. 278 (1997) 35.
[16] R.K. Singh, P. Bhriguvansh, B.P. Asthana, A.L. Verma, Chem. Phys. Lett. 296 (1998) 611.
[17] R.K. Singh, S.K. Srivastava, A.K. Ojha, U. Arvind, B.P. Asthana, J. Raman Spectrosc. 37 (2006) 76.
[18] S.K. Srivastava, A.K. Ojha, P. Raghuvansh, W. Kiefer, B.P. Asthana, J. Raman Spectrosc. 37 (2006) 1287.
[19] S.K. Srivastava, A.K. Ojha, P.K. Sinha, B.P. Asthana, R.K. Singh, J. Raman Spectrosc. 37 (2006) 68.
[20] A. Morresi, L. Mariani, M.R. Distefano, M.G. Giorgini, J. Raman Spectrosc. 26 (1995) 179.
[21] B.P. Asthana, W. Kiefer, in: J.R. Durig (Ed.), Vibrational Spectra and Structure, vol. 20, Elsevier, Amsterdam, 1993, p. 67.
[22] A.F. Bondarev, A. Mardaeva I, Opt. Spectrosc. 35 (1973) 167.
[23] S.F. Fischer, A. Laubereau, Chem. Phys. Lett. 55 (1978) 189.
[24] G. Döge, R. Arndt, A. Khuen, Chem. Phys. 21 (1977) 53.
[25] D.W. Oxtoby, Adv. Chem. Phys. 40 (1979) 1.
[26] P.A. Egelstaff, An Introduction to the Liquid State, Academic Press, New York, 1967
[27] F. Billes, H. Mikosch, Acta Chim. Hung. 130 (1993) 901.
[28] F. Billes, H. Mikosch, S. Holly, THEOCHEM 423 (1998) 225.
[29] J.M.L. Martin, C.V. Alsenoy, J. Phys. Chem. 100 (1996) 6973.
[30] A.D. Boese, J.M.L. Martin, J. Phys. Chem. A 108 (2004) 3085.
[31] K.V. Berezin, P.M. Nechaev, El'kin, Russ. J. Phys. Chem. 79 (2005) 425.
[32] K.S. Kim, J.Y. Lee, H.S. Choi, J. Kim, J.H. Jang, Chem. Phys. Lett. 266 (1997) 497.
[33] H.S. Gutowsky, T. Emilsson, E. Arunan, J. Chem. Phys. 99 (1993) 4883.
[34] P. Hobza, V. Spirko, H.L. Selzle, E.W. Schlag, J. Phys. Chem. A 102 (1998) 2501.
[35] W. Caminati, P. Moreschini, P.G. Favero, J. Phys. Chem. A 102 (1998) 8097.
[36] W. Caminati, L.B. Favero, P.G. Favero, A. Maris, S. Melandri, Angew. Chem., Int. Ed. Engl. 37 (1998) 792.
[37] S. Melandri, M.E. Sanz, W. Caminati, P.G. Favero, Z. Kisiel, J. Am. Chem. Soc. 120 (1998) 11504.
[38] M.J. Frisch, Gaussian 03, Revision A.1, Gaussian, Inc., Pittsburgh, PA, 2003.
[39] R. Dennington Jr., T. Keith, J. Millam, K. Eppinnett, W.L. Hovell, R. Gilliland, GaussView 4.1, Gilliland R. Semichem, Inc., Shawnee Mission, KS, 2003.
[40] E.D. Glendening, A.E. Reed, J.E. Carpenter, F.A. Weinhold, NBO, Version 3.1, 1995.
[41] J.G. Kirkwood, J. Chem. Phys. 2 (1934) 351.
[42] E. Cance's, B. Mennucci, J. Tomasi, J. Chem. Phys. 107 (1997) 3032.
[43] B. Mennucci, E. Cance's, J. Tomasi, J. Chem. Phys. B 101 (1997) 10506.
[44] A.D. Becke, J. Chem. Phys. 98 (1993) 5648.
[45] C. Lee, W. Yang, R.G. Parr, Phys. Rev. B 37 (1988) 785.
[46] S.F. Boys, F. Bernardi, Mol. Phys. 19 (1990) 553.
[47] (a) J.A. Pople, A.P. Scott, M.W. Wong, L. Radom, Israel J. Chem. 33 (1993) 345;
(b) G. Rauhut, R. Pulay, J. Phys. Chem. 99 (1995) 3093;
(c) A.P. Scott, L. Radom, J. Phys. Chem. 100 (1996) 16502;
(d) P.L. Fast, J. Corchado, M.L. Sánchez, D.G. Truhlar, J. Phys. Chem. A 103 (1999) 3139.
[48] C. Cappelli, C.O. Silva, J. Tomasi, J. Mol. Struct. (THEOCHEM) 544 (2001) 191.
[49] S. Breda, I.D. Reva, L. Lapinski, M.J. Nowak, R. Fausto, J. Mol. Struct. 786 (2006) 193–206.
[50] P. Hobza, Z. Havlas, Chem. Rev. 100 (2000) 4253–4264.
[51] S.C. Wang, P.K. Sahu, S.L. Lee, Chem. Phys. Lett. 406 (2005) 143–147.
[52] J.R. Grigera, J. Chem. Phys. 114 (2001) 8064.
[53] B. Tomberli, C.J. Benmore, P.A. Egelstaff, J. Neuefeind, V. Honkimäki, J. Phys. Condens. Matter 12 (2000) 2597.
[54] G.S. Kell, in: F. Franks (Ed.), Water. A Comprehensive Treatise, Plenum, New York/London, 1972, p. 1.
[55] R.K. Singh, B.P. Asthana, P.R. Singh, T. Chakraborty, A.L. Verma, J. Raman Spectrosc. 29 (1998) 561.
[56] A.K. Ojha, S.K. Srivastava, R.K. Singh, B.P. Asthana, J. Phys. Chem. A 110 (2006) 9849.
[57] R.K. Murray, D.K. Granner, P.A. Mayes, V.K. Mayes, Harper's Illustrated Biochemistry, International Edition, 2003.